

S. Newman

Department of Cell Biology
and Anatomy
New York Medical College
Valhalla, NY 10595, USA

M. Cloître*

C. Allain

Laboratoire FAST
Bâtiment 502
Université Paris-Sud
91405 Orsay Cédex, France

G. Forgacs

Departments of Physics
and Biology
Clarkson University, Potsdam,
NY 13699-5820, USA

D. Beysens

Département de Recherche
Fondamentale
sur la Matière Condensée
CEN Grenoble
38054 Grenoble Cedex 9,
France

Viscosity and Elasticity During Collagen Assembly In Vitro: Relevance to Matrix-Driven Translocation

In order to better understand the gelation process associated with collagen assembly, and the mechanism of the in vitro morphogenetic phenomenon of "matrix-driven translocation" [S. A. Newman et al. (1985) Science, 228, 885–889], the viscosity and elastic modulus of assembling collagen matrices in the presence and absence of polystyrene latex beads was investigated. Viscosity measurements at very low shear rates ($0.016\text{--}0.0549\text{ s}^{-1}$) were performed over a range of temperatures ($6.9\text{--}11.5^\circ\text{C}$) in a Couette viscometer. A magnetic levitation sphere rheometer was used to measure the shear elastic modulus of the assembling matrices during the late phase of the gelation process. Gelation was detected by the rapid increase in viscosity that occurred after a lag time t_L that varied between 0 and ~ 500 s. After a rise in viscosity that occurred over an additional ~ 500 s, the collagen matrix was characterized by an elastic modulus of the order of several Pa. The lag time of the assembly process was relatively insensitive to differences in shear rate within the variability of the sample preparation, but was inversely proportional to the time the sample spent on ice before being raised to the test temperature, for test temperatures $>9^\circ\text{C}$. This suggests that structures important for fibrillo-

Received April 23, 1996; accepted July 2, 1996.

* Present address: Unité Mixte de Recherche, CNRS/Elf-
Atochem, Centre d'Application, 92330 Lavallois-Perret Cedex,
France.

Biopolymers, Vol. 41, 337–347 (1997)

© 1997 John Wiley & Sons, Inc.

CCC 0006-3525/97/030337-11

genesis are capable of forming at 0°C. The time dependence of the gelation process is well-described by an exponential law with a rate constant $K \sim 0.1 \text{ s}^{-1}$. Significantly, K was consistently larger in collagen preparations that contained cell-sized polystyrene beads. From these results, along with prior information on effective surface tension differences of bead-containing and bead-lacking collagen matrices, we conclude that changes in matrix organization contributing to matrix-driven translocation are initiated during the lag phase of fibrillogenesis when the viscosity is ≤ 0.1 Poise. The phenomenon may make use of small differentials in viscosity and/or elasticity, resulting from the interaction of the beads with the assembling matrix. These properties are well described by standard models of concentrated solutions.

© 1997 John Wiley & Sons, Inc.

INTRODUCTION

Cells in the connective tissues of multicellular organisms produce their own complex environment known as the extracellular matrix (ECM; for a review on the subject, see Ref. 1). The most abundant organic component of the ECM is type I collagen, a rod-like protein that assembles into macromolecular fibrils and subsequently into fibers and macroscopic fiber bundles.^{2,3} “Irregular” connective tissues, which include the dermis of the skin, the capsules of most organs, and the loose mesenchymes from which many structures form during embryonic development, must have the capacity to resist stresses in all directions, and consequently contain collagen fibers and/or fiber bundles organized into random networks.

Networks of type I collagen also form *in vitro*. The protein first assembles into fibers, which as they elongate, intermesh with each other and eventually form a gel.³ The gelation process in collagen, like that in other macromolecular systems, has been analyzed in terms of the formation of random “percolation networks.”^{4–7} However, despite extensive studies of this assembly process and the physical phenomena accompanying it,^{3,8–13} a number of fundamental questions remain unanswered. For instance, the nature of intermediate forms during collagen fibrillogenesis remains controversial,³ leading to uncertainty with respect to the scale on which macroscopic structure formation occurs.

The formation of collagen networks may have a bearing on the morphogenesis of connective tissues. It has long been hypothesized that tissues of different origin can behave as immiscible fluids.^{14–16} That is, contiguously placed tissues will fail to exchange cells along their common boundary despite the fact that the cells are entirely mobile within each tissue mass. The origin of this apparent phase separation in epithelioid tissues, in which cells make direct contact with each other, is well understood.^{17–19} In contrast, the basis for such phenomena in connective tissues is obscure. Recently, a set of experimental

results on a model connective tissue system has provided some insight into this question.^{6,20,21} The system consists of solutions of assembling fibers of type I collagen. One such solution (phase 1) contains $>2.5 \times 10^6$ uniformly suspended cell-sized ($6 \mu\text{m}$) polystyrene latex beads per cm^3 , while the other solution (phase 2) is prepared without beads. When droplets of the two fluids, with collagen concentrations in excess of 1.5 mg/mL , are placed contiguously to one another on a polystyrene substratum (or alternatively, injected into the opposite ends of a chamber consisting of two parallel polystyrene plates separated by 0.2 cm), a sharp interface forms between the two fluids. The development of this interface coincides with the bulk flow of phase 1 above and below phase 2, leading to translocation of the beads (Figure 1). Movement stops after a few minutes. The typical velocity v of translocation is $2 \times 10^{-3} \text{ cm/s}$.

This phenomenon, termed “matrix-driven translocation” (MDT),^{20,21} was proposed to depend on a driving force resulting from the difference in the effective interfacial tensions between the two phases⁶:

$$F = \gamma L \quad (1)$$

with L being the contact line between the phases, $\gamma = \sigma_{w2} - \sigma_{w1} - \sigma_{12}$ the spreading coefficient,²² σ_{w1} and σ_{w2} the effective interfacial tensions between the respective phases and their bounding substrata (polystyrene and air, or the two polystyrene plates), and σ_{12} the effective interfacial tension between phases 1 and 2. The separation of phases was hypothesized to be the consequence of early events in an assembly process that eventually leads to the gelation of collagen by virtue of the formation of a static percolation network.^{5,23} In particular, the beads were proposed to interact with the dynamical percolation network assumed to be present in the collagen solution prior to its gelation, resulting in a phase thermodynamically distinct from pure colla-

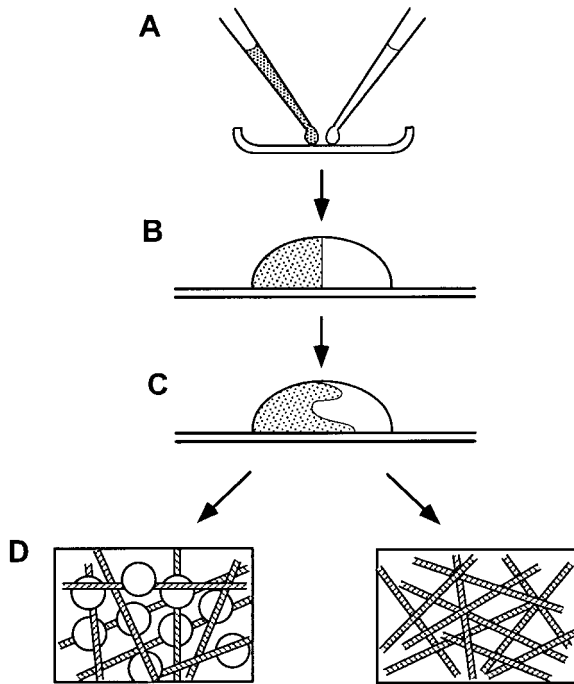


FIGURE 1 Diagrammatic representation of matrix-driven translocation (MDT) assay. (A) The deposition on the surface of a petri dish of two droplets of soluble type I collagen, one containing and one lacking cells, or cell-sized polystyrene latex beads. (B) A higher magnification schematic representation of a side view of the two droplets shortly after their fusion. (C) The translocation effect—a reconfiguration of the apparent interface between the two droplets during the collagen assembly process. (D) A higher magnification schematic view of the growing collagen fibrils shown in C, disrupted by beads or cells on the left, and forming a pervasive network on the right.

gen.⁷ The two phases should thus exhibit a nonzero effective interfacial tension σ_{12} . (We use the term “effective interfacial tension” throughout this work, since as gelation proceeds the collagen-based phases are elasticoviscous liquids, and their surface free energies contain an elastic component.²⁴) Detailed measurement of the tensions at the air–liquid interface have indeed detected a difference $\sigma_{w2} - \sigma_{w1}$ of a few dynes/cm, with little time dependence.²⁵

In the present work we report the results of measurements of the viscoelastic properties of assembling collagen matrices in the absence and presence of suspended polystyrene latex beads. In consideration of the fact that gelation is a second-order phase transition,^{23,26} in which viscosity increases indefinitely below the transition, and well-defined mechanical properties appear above it, our study had

two objectives. First, we sought to follow the behavior of the viscosity and elastic modulus during and after the gelation of collagen, and relate these properties to the scaling theory of second-order phase transitions. Second, in order to better understand the physical processes underlying MDT, we sought to relate the development of any viscoelastic differences between the two phases to the previously measured values of the effective tensions.²⁵ For this purpose we performed viscosity measurements over a range of temperatures and shear rates, in both phases 1 and 2. Similar to previous studies,⁸ we found that a rapid increase in viscosity starts only after a lag time t_L , but unexpectedly observed that the lag time varied inversely with the amount of time the collagen sample spent on melting ice after its pH and ionic strength were adjusted to physiological values. This implies that important early steps of fibrillogenesis, with no apparent effect on viscosity, can occur at 0°C. We also found that the presence of as few as one 6 μm diameter polystyrene bead per $2.2 \times 10^5 \mu\text{m}^3$ significantly accelerated the increase in viscosity from the earliest stages of the gelation process.

From these results we conclude that the phase organization and separation seen in MDT is probably based on the formation of macroscopic structures by collagen fibrils that arise mainly during the lag phase. Translocation itself is most likely initiated by wetting forces during the lag phase, or shortly thereafter, when the viscosities are less than 10^2 Poise. The continuation of translocation may be the consequence of differences in viscosity and/or elasticity of the two solutions as fibrillogenesis proceeds.

EXPERIMENTAL PROCEDURES

Preparation of Collagen Solutions

Type I collagen was extracted from the tails of young adult rats as described.²⁰ The acetic acid extract was adjusted to a protein concentration of 3–5 mg/mL and dialyzed for 2 days against two changes of 0.1 strength Ham’s F-12 medium without bicarbonate (Life Sciences, Grand Island, NY). Phase 1 was prepared by starting with 0.7 mL dialyzed collagen solution on ice and adding in succession, with rapid mixing, 0.1 mL 9.3×10^6 Ham’s F-12, 0.1 mL distilled water, and 0.1 mL sodium bicarbonate (11.76 mg/mL). This, in turn, was rapidly mixed with 1 mL of complete Ham’s F-12 containing 9×10^6 polystyrene latex beads (6 μm ; Polysciences, Warrington, PA) per mL. Phase 2 was prepared as above, but with 1 mL F-12 without suspended beads. All experiments were

therefore performed with collagen in 1× strength tissue culture medium, the conditions under which the MDT effect has been best characterized.^{20,21} The collagen samples were kept on ice for controlled amounts of time until being transferred to the viscometer or rheometer described below.

The Couette Viscometer

We used a conventional Couette viscometer (Contraves Low Shear 30) with imposed shear rates. This instrument consists of two coaxial cylinders separated by a gap of about 0.5 mm. When the outer cylinder is set into rotation the torque on the inner cylinder is proportional to the viscosity. The gap between the cylinders was filled with the sample and the viscosity was recorded as a function of time until it reached the maximum value detectable by the apparatus. The shear rate S , was set to a value between 10^{-2} s^{-1} and $5 \times 10^{-2} \text{ s}^{-1}$ depending on the experiment, and was held constant during each run. The measured viscosity values were between 10^2 and 10^3 Poise. Temperature was controlled by a thermostated circulating water bath and was maintained constant to within 0.1°C . On the basis of the gap size in the viscometer and the heat diffusivity in aqueous solutions, we estimate the temperature equilibration times in our experiments to be on the order of 10 s.

The Magnetic Levitation Sphere Rheometer

The elastic modulus was measured using a specially designed magnetic levitation sphere rheometer (MLSR).^{27–30} The principle of the apparatus is the following: a small magnetic sphere (0.8 mm in diameter) is kept suspended motionless in a vertical cylindrical tube 10 mm in diameter (the test cell) filled with the collagen solution, by means of a monitored magnetic field. The test cell is vertically translated at a variable speed between $5 \times 10^{-3} \text{ mm/s}$ and $5 \times 10 \text{ mm/s}$. The shear rate is defined as the velocity divided by the sphere diameter, and can be as low as 10^{-2} s^{-1} . The total relative deformation can be made as little as 10^{-2} . The rheological properties of the sample are deduced from the intensity of the current in the coil that produces the magnetic field keeping the sphere motionless. Before gelation the sample is viscous and the intensity of the current is proportional to the viscous force exerted on the sphere by the flow around it, i.e., to the velocity of translation. The viscosity of the solution is obtained from the coefficient of proportionality. After gelation the sample exhibits elasticity and the intensity of the current is proportional to the total displacement of the tube. The proportionality constant is then related to the shear elastic modulus.

In each run the test cell was filled with a collagen sample before inserting it in the apparatus. The temperature of the cell was maintained at 11.5°C with a thermostated circulating water bath. The measurements were

begun once the magnetic sphere was suspended motionless in the magnetic field. The test cell was moved sequentially for short periods ($<100 \text{ s}$) with the velocity and duration of displacement being modified at each measurement, considering the result of the previous one. This protocol allowed the perturbation of the sample during gelling to be minimized, and permitted determination of the steady state properties of the gelling collagen.

RESULTS

Viscosity Measurements

A typical run with the Couette viscometer is shown in Figure 2. Time is measured from the removal of the collagen from ice. The two sets of points refer, respectively, to experiments with pure collagen and with collagen plus beads. We observed three time regimes:

(a) time = $[0 - t_L]$. During this period the viscosity does not vary much and remains lower than 0.1 Poise for both the collagen and collagen plus beads preparations. The time t_L is the well-known lag time seen in previous studies in which turbidity³¹ or viscosity⁸ were monitored. In the present studies this lag time was variable from experiment to experiment, ranging between 0 and 10 min, with no consistent dependence of t_L on shear rate (in the range $10^{-2} \text{ s}^{-1} \leq S \leq 5 \times 10^{-2} \text{ s}^{-1}$), or on the presence or absence of beads. Within a given set of runs, however, there was a strong inverse dependence of t_L on the time the sample spent on ice (t_i) prior to being poured into the viscometer. The result of an experiment aimed at probing this dependence is shown in Figure 3. Additional experiments conducted in the range $9.2\text{--}11.5^\circ\text{C}$ gave similar results (not shown). For experiments performed at these temperatures there was no lag phase when t_i exceeded 300 s, and the viscosity immediately after removal from ice was larger than 0.1 Poise.

A different situation held, however, for experiments performed at 6.9°C , the lowest temperature studied. Here the lag times were longer, typically 10 min for a t_i of 2 min (as compared to a t_L of about 5 min for a t_i of 2 min at 11.5°C), and were not substantially shortened by prolonging t_i to 10 min.

(b) time = $[t_L - t_S]$. After the lag time the viscosity increases rapidly, with exponential kinetics (see below), characterized by a rate constant K ranging between 0.03 and 0.16 s^{-1} , until a ‘bump’ appears in the curve for the bead-containing preparation at $t = t_S$ (Figure 2). For six out of seven sets of measurements in which bead-lacking and bead-containing collagen solutions were kept on ice for

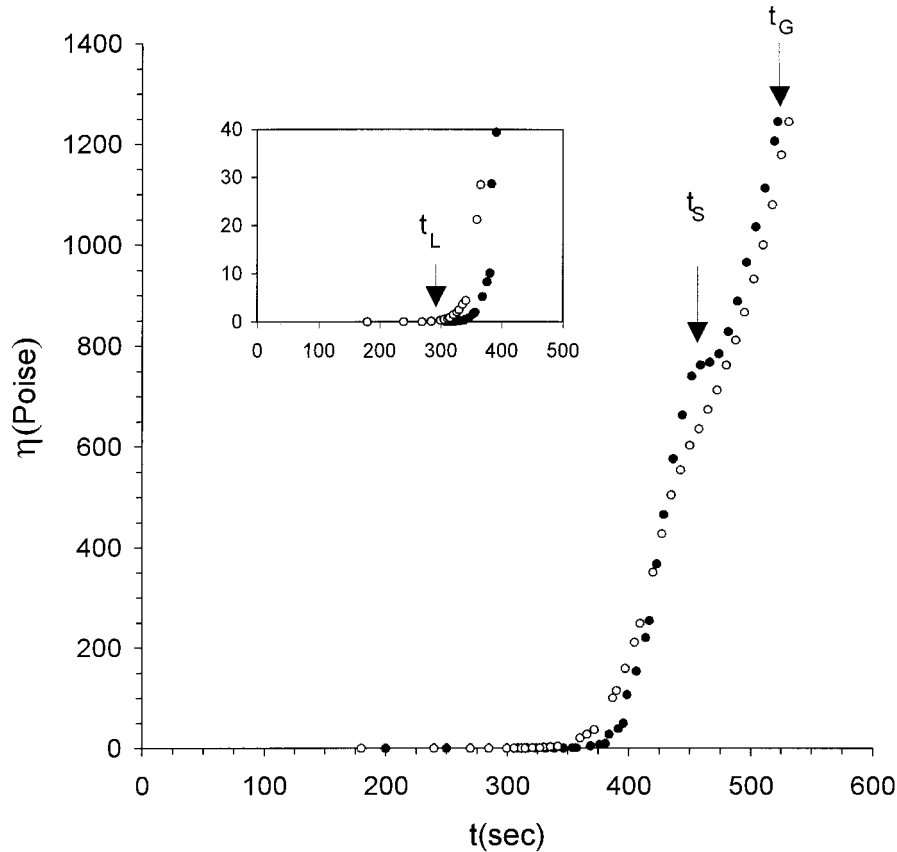


FIGURE 2 A typical viscosity run in the Couette viscometer for pure collagen (open symbols) and collagen plus beads preparation (solid symbols). Shear rate: 0.0219 s^{-1} ; $T = 11.5^\circ\text{C}$; the time the preparations spent on ice, $t_i = 120 \text{ s}$. For the meaning of t_G , t_L , and t_S , see text. The inset shows in more detail the behavior of the viscosity at the onset of gelation. (Note the scale of the vertical axis.)

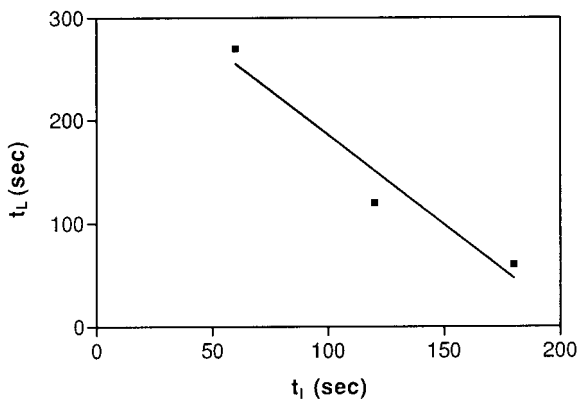


FIGURE 3 The dependence of the lag time t_L on the time the preparations spent on ice t_i , prior to the viscosity measurement. The three points shown correspond to measurements performed at 11.5°C with the same collagen preparation (which differed from the one used in the viscosity measurements shown in Figure 2).

identical times before analysis in the Couette apparatus ($t_i = 2 \text{ min}$), and the lag times for the paired preparations were within a factor of 1.5 of each other, we found that K was 1.3–2-fold greater for the bead-containing than the bead-lacking preparation. This included experiments performed at 6.9°C at a shear rate of 0.0161 s^{-1} , and at 11.5°C with shear rates of 0.0219 , 0.0237 , and 0.0549 s^{-1} . In the case that did not conform to this pattern, the K values for the two preparations were within 10% of each other. We interpret the bump as indicating the disruption of the gel network by the shear flow; the fact that it was always present or more prominent in the bead-containing preparation is consistent with the kinetic results suggesting that the beads nucleated the gelation process (see below).

(c) time = $[t_S - t_G]$. Gelation proceeds in the presence of shear. During this phase the viscosity becomes very large ($>100 \text{ Poise}$). After a time $t_G \geq 500 \text{ s}$ the viscosity ceases to rise and gelation can be considered to be completed. At this point

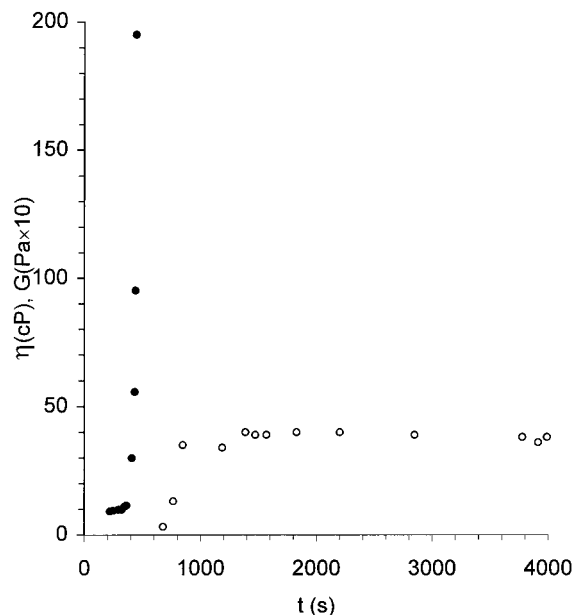


FIGURE 4 Experimental results obtained with the magnetic levitation sphere rheometer. The curves show the increase of the viscosity η (solid symbols) and elastic modulus G (open symbols) near the gel point. Only results obtained with a bead-free solution are shown; bead containing solutions gave similar results.

the system is characterized by an elastic modulus (see below). The shear rate had a pronounced effect on the final viscosity achieved by the system; the viscosity typically reached 1800 Poise for a shear rate S of 0.016 s^{-1} , 1300 Poise for $S = 0.0219 \text{ s}^{-1}$, 1000 Poise for $S = 0.0297 \text{ s}^{-1}$, and 300 Poise for $S = 0.0549 \text{ s}^{-1}$. The presence of beads had no apparent effect on the terminal viscosity.

Elasticity Measurements

The MLSR, in principle, enables both the viscosity and elastic modulus to be measured during the same run. Although it was difficult to observe the early portion of the viscosity curves because the time necessary to assemble and calibrate the apparatus at the beginning of each run, the later viscous behavior monitored by this method was consistent with the Couette measurements. Once the gelation time t_G had been reached, a shear elastic modulus (G) developed and saturated at a constant value (Figure 4). The plateau values of G correspond to the completion of the gelation process, and were scattered between about 1.5 and 6 Pa for various preparations. The reason for the scatter is unclear: it could reasonably be attributed to the sensitivity of the gel net-

work to the initial conditions, e.g., the preparation of the sample and its history. In any case, the data in Figure 4 indicate that the shear elastic modulus, like the terminal viscosity, does not show a dependence on the presence of beads that exceeds the dispersion due to sample history.

THEORETICAL CONSIDERATIONS

Percolation and Collagen Fibrillogenesis

It is only during the time period $[t_L - t_S]$ that the viscous behavior can be analyzed using the current theory of gelation, which is based on percolation.⁵ According to this theory, the viscosity varies as a power of the conversion factor⁴ p :

$$\frac{\eta}{\eta_0} \sim \left(1 - \frac{p}{p_c}\right)^{-x} \quad (2)$$

The conversion factor is assumed to be zero and one, respectively, at the beginning and the end of the gelation process and is related to the number of effective links N between fibers: $p/p_c = N/N_G$. Here N_G (which defines p_c , the critical value of the conversion factor) is the number of links at the gelation threshold, when a percolating network of links connects the entire sample. In Eq. (2) η_0 is the viscosity of the sample just after preparation. The measured values of the exponent x above vary between 0.6 and 1.5.⁵ All the previous experimental data for x have been obtained by considering the time dependence of the gelation process. The gel phase is considered to be reached at the time t_G , when $N = N_G$. According to the specific process that causes the formation of a link, one may find different time dependencies for N . As a first approximation,²⁹ N is taken to be proportional to the time, $N \sim t$, so that

$$\frac{\eta}{\eta_0} \sim \left(1 - \frac{t}{t_G}\right)^{-x} \quad (3)$$

In Figure 5, we plot $(\eta/\eta_0)^{-1/x}$ as a function of time for different values of the exponent x . When Eq. (3) holds, $(\eta/\eta_0)^{-1/x}$ should vary linearly with t . However, even for values of x that are unrealistically large when compared with the exponent expected for percolation ($x = 0.6-1.5$), the variations of $(\eta/\eta_0)^{-1/x}$ with respect to time are not straight lines in the vicinity of the gel point.

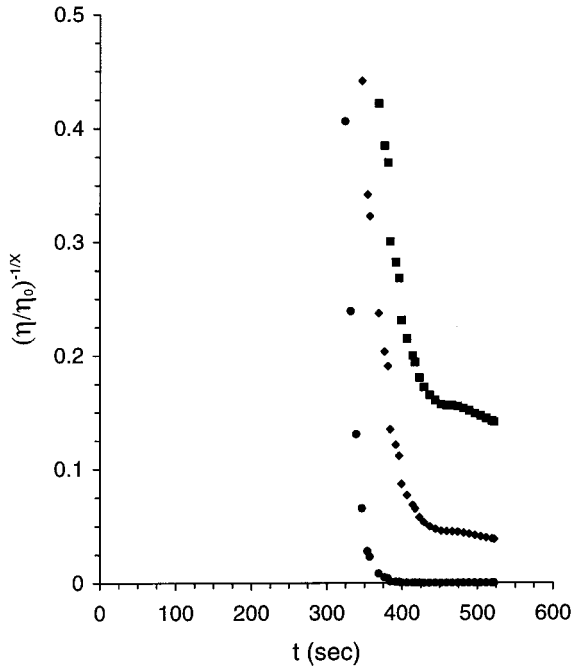


FIGURE 5 Representation of $(\eta/\eta_0)^{-1/x}$ for the same preparation as in Figure 2. For clarity, we only display the data corresponding to pure collagen. The collagen plus bead preparation gives similar variations. We have considered three values of the exponent x : 0.9 (circles), 3 (diamonds), and 5 (squares).

In the case of the gelation of denatured collagen, however, it has been reported³² that the number of links formed in the course of time is well described by an exponential dependence. Accordingly, we assume that N varies as

$$N \sim N_0[1 - e^{-\kappa(t-t_L)}], \text{ for } t \geq t_L \quad (4)$$

where t_L is the lag time as before and κ is a characteristic rate constant. Assuming that $N_0 \sim N_G$, one arrives at

$$\frac{\eta}{\eta_0} \sim \exp[K(t - t_L)] \quad (5)$$

where [using $p/p_c = N/N_G$, and Eqs. (2) and (4)] $K = \kappa x$.

Figure 6 is a semilogarithmic plot of η/η_0 as a function of time for the experiment corresponding to Figure 2. In the time interval $[t_L, t_s]$, the experimental points both for phases 1 and 2 fall on straight lines, which supports the behavior described by Eq. (5), with an exponential time dependence of link formation. Matching the experimental curves for the viscos-

ity with an exponential [Eq. (5)] yields $0.04 \text{ s}^{-1} < K < 0.1 \text{ s}^{-1}$. Provided percolation adequately describes collagen fibrillogenesis, using the above values of x together with our experimental results, we predict that κ ranges between 0.03 and 0.16 s^{-1} .

Nucleation and Collagen Fibrillogenesis

As discussed earlier, we have systematically observed that the rate constant, K is larger for the bead containing solution than for the pure collagen solution. Since the rise of the viscosity curve is sharper for the bead containing phase at the beginning of the gelation process (see inset to Figure 2), the difference between the viscosities for the two preparations also increases in this regime. These observations are consistent with the elementary theory of viscosity behavior in solutions.³³

The surface of the polystyrene beads contain heparin-like moieties,³⁴ which are known to have high affinity for collagen.³⁵ The beads can then act as nucleation centers for collagen fibrillogenesis, and we suggest this accounts for the higher K values of the bead containing phase. According to Einstein's theory³⁶ the zero shear viscosity of a solution of particles increases with the volume fraction, ϕ of the particles as $\eta/\eta' = 1 + 2.5\phi$. This result is exact for small values of ϕ (<0.05). Here η' is the viscosity in the absence of particles. As fibrillogenesis proceeds and more fibrils surround the individual beads, their effective volume increases, leading

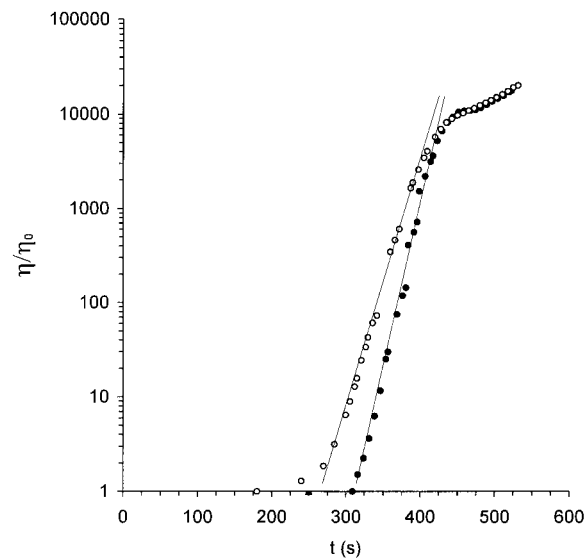


FIGURE 6 Representation of $\log(\eta/\eta_0)$ vs t for the same preparations as in Figure 2. The straight lines were used to determine the value of the rate constant K .

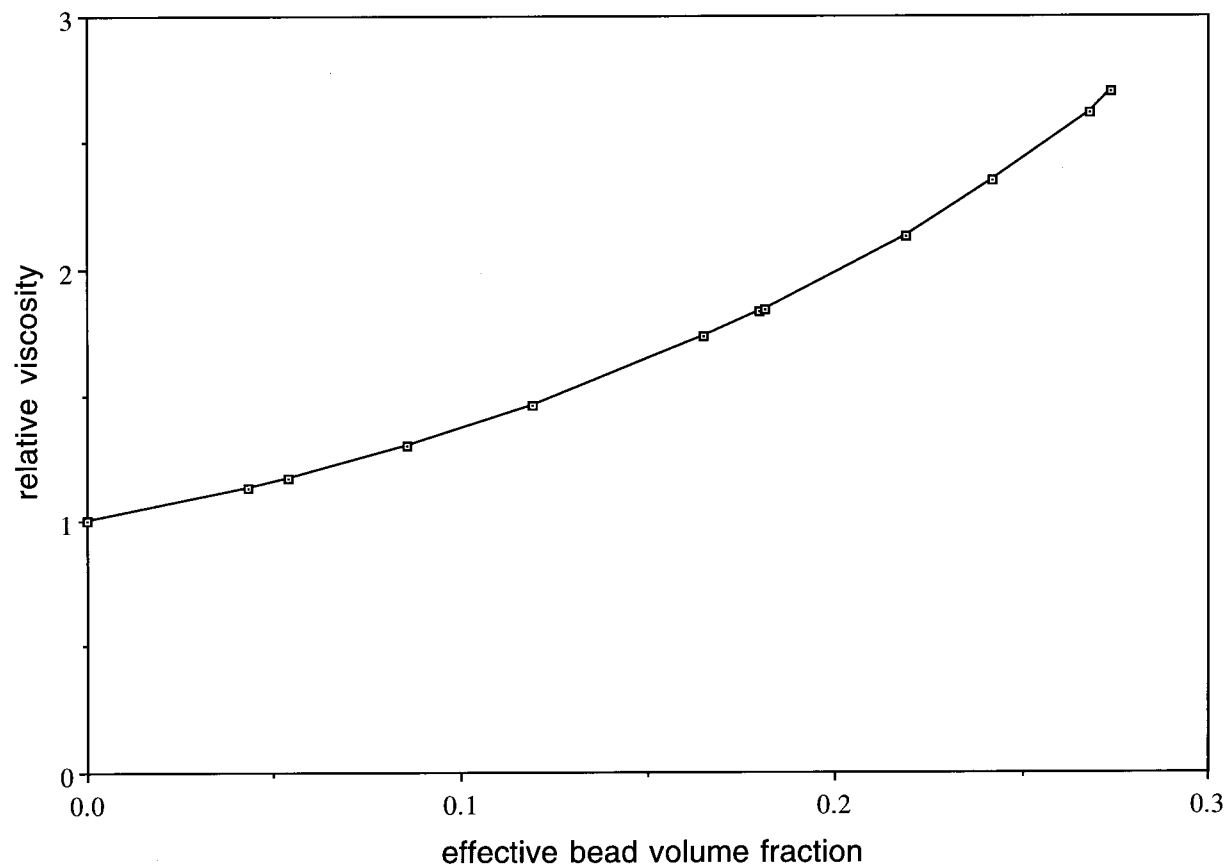


FIGURE 7 Variation of the relative viscosity η/η' as a function of the effective bead concentration derived using Thomas' expression. Here η and η' denote, respectively, the viscosity of the bead containing and bead-free collagen solution.

to the increase of the effective volume fraction ϕ_{eff} and Einstein's expression is no longer applicable. For larger volume fractions of solute particles many expressions have been proposed for the ϕ dependence of the relative viscosity.^{33,36} Most of these give similar results in the interval $0 < \phi < 0.5$. Here, for the quantitative analysis of our data we use Thomas' phenomenological formula,³⁷ well known in engineering applications:

$$\eta/\eta' = 1 + 2.5\phi + 10.05\phi^2 + 0.00273 \exp(16.6\phi) \quad (6)$$

The above expression is valid for $0 < \phi < 0.55$.³⁷ Using our experimental results for η and η' in the time interval $[t_L - t_S]$ (see Figure 2), inverting Thomas' formula we have determined the effective volume fraction of the latex particles. The resulting curve is plotted in Figure 7. The corresponding time dependence of ϕ_{eff} is shown in

Figure 8. The original volume fraction of the 6 μm beads is very small, being $\sim 10^{-5}$, and not surprisingly the experimental results, during the initial rise of the viscosity in Figure 7 can be fitted extremely accurately to Einstein's exact expression. As the solutions approach the gelation point the viscosities increase to very large values and the contribution of beads should not be significant. Indeed, the initial difference in the viscosities disappears at the later stage of the gelation process (see Figure 2). The graph in Figure 8 suggests that the increase of ϕ_{eff} indeed can be interpreted as that due to the accumulation of fibrils around beads. The linear time dependence of ϕ_{eff} implies that in the interval $[t_L, t_S]$ the effective bead radius grows as $t^{1/3}$. This growth law is identical to that observed in many diffusion-induced growth processes, in particular for the typical radius of drops formed by the low volume fraction component in phase separating binary fluids.³⁸

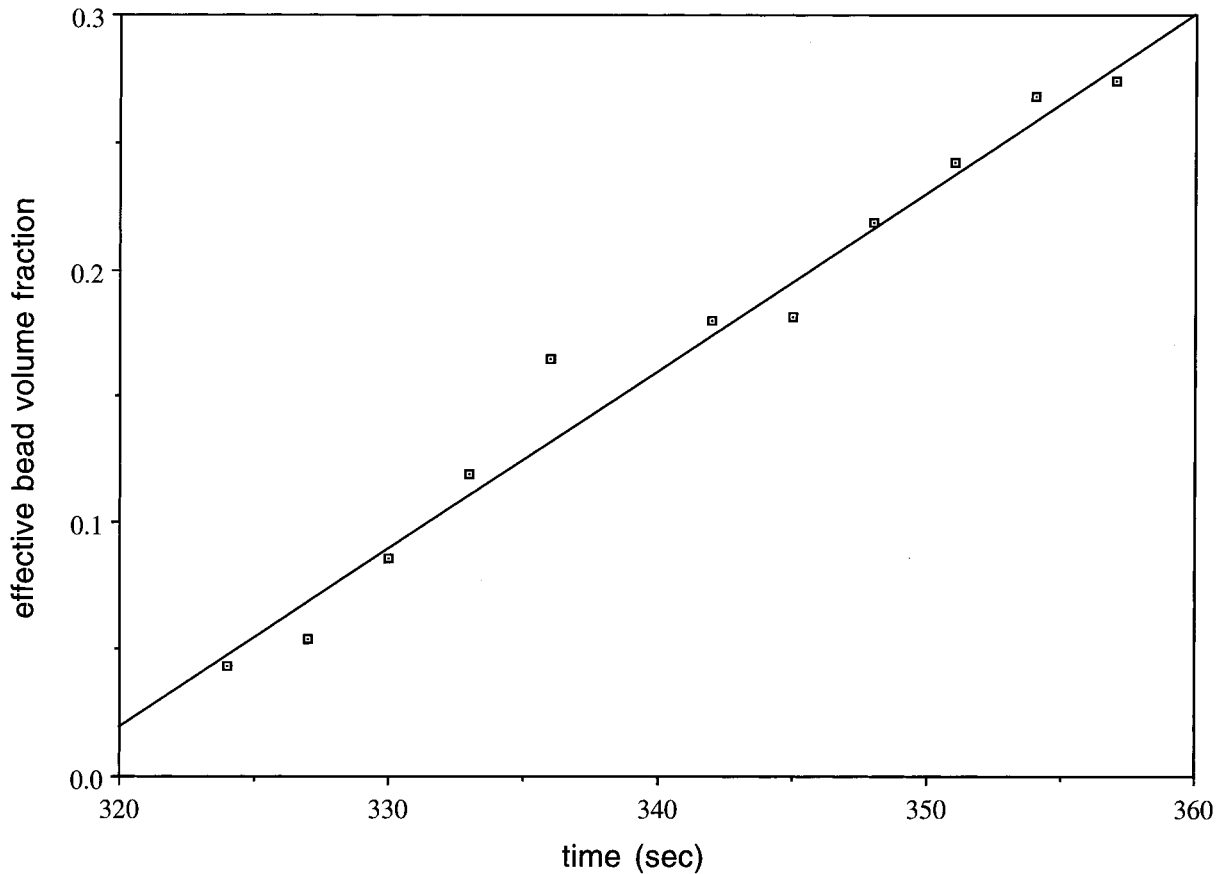


FIGURE 8 Time dependence of the effective bead concentration obtained by combining the experimental results for the relative viscosity with Thomas' expression.

DISCUSSION

The motivation for this work was two-fold. On one hand we sought to measure systematically the time evolution of the viscosity of collagen solutions during the process of gelation and interpret the results in terms of the modern theory of this process.²⁹ On the other hand, we were interested in relating the results of our earlier studies on the interfacial properties of such solutions²⁵ to information on viscosity, in order to get a better theoretical understanding of the phenomenon of MDT.²⁰

With respect to collagen gelation, our experiments have led to the identification of two novel effects. First, while it has long been known that small-scale assembly events, with no measurable effect on viscosity or optical density, take place during a temperature-dependent lag phase, our results suggest that in addition there are microscopic nucleation events occurring at 0°C that are distinct from those that occur during lag phase. These processes are distinguishable by virtue of the fact that

extended periods on ice substantially shortened the lag phase for assays performed at 9.2–11.5°C, but they had no impact on the length of the lag phase if fibrillogenesis was assayed at 6.9°C. It is possible that assembly intermediates that form at 0°C require collisions in order to be converted into productive nuclei, and that the kinetic energy needed for this is not available at 6.9°C. These two processes may correspond to the primary and secondary nucleation events hypothesized by Piez.³⁹

The second novel finding in our fibrillogenesis studies is that polystyrene latex beads appear to be able to act as nucleation centers for collagen assembly. Our inference that this is the case is based on two independent factors. First, we observed an initial acceleration of fibrillogenesis in the presence of a very dilute suspension of particles, reflected in larger K values, in the period just after the lag phase has been completed. Second, we were able to account for the greater viscosities of the bead-containing relative to bead-free solutions in the interval $[t_L, t_S]$, by the assumption that the effective bead diameter increases

with time. We suggest that this effect may be caused by the nucleation of collagen assembly by the polystyrene beads, and its deposition on their surfaces. Commercial polystyrenes have been found to be excellent mimics of the glycosaminoglycan heparin in its capacity to interact with proteins.³⁴ Moreover, previous studies on the interaction of heparin with type I collagen indicate that the glycosaminoglycan causes assembly into fibrils of increased stability at the expense of lower stability structures including nonassociated molecules and thin fibrils.³⁵ This hypothesized recruitment of collagen to the bead surface may provide a basis for the bead-induced alteration in network structure of the assembling collagen matrix suggested to underlie MDT.⁷

While previous analyses have suggested that MDT results from an imbalance in the surface and interfacial tensions between the bead-containing and bead-free collagen droplets,^{6,7} the magnitudes of the viscosities of these solutions clearly place constraints on the efficacy of this mechanism. The previously measured difference in surface tension between the bead-containing and bead-free collagen solutions²⁵ implies that there would be a nonzero value for the spreading coefficient at their mutual interface. If spreading is to drive MDT, this coefficient must be sufficiently large to transport fluids of progressively increasing viscosity over macroscopic distances.

Assuming that MDT indeed is driven by forces originating from a nonzero spreading coefficient [see Eq. (1)], we can establish an energy balance equation for our system that takes into account the measured values of the viscosity. On one hand, we estimate the energy dissipation per unit volume and time due to viscous effects as $\eta(v/e)^2$, where $e = 0.2$ cm, is the typical thickness of spreading collagen droplets (see Figure 1). On the other hand, a nonzero interfacial tension between the two solutions implies that during MDT an amount of work, γLvt , is performed. Considering, in addition, that $e \sim L$ and that the dissipating volume is $\sim e^3$, equating the energy dissipation with the work of surface and interfacial forces, we arrive at

$$\gamma = \eta v \quad (7)$$

The same result follows directly from the dimensional analysis of the Navier-Stokes equation (NSE). For small and slowly varying flow velocities the pressure term and the viscous term in NSE are of the same order of magnitude, $\nabla P \sim \eta \Delta v$ (where ∇ and Δ are the gradient and Laplace opera-

tors, respectively). Since $\nabla \sim 1/e$ and $P \sim \gamma/e$, the above relationship between γ and η follows. As the viscosity is increasing in time from the end of the lag phase, MDT can proceed as long as

$$\sigma_{w2} - \sigma_{w1} - \sigma_{12} \geq \eta v \quad (8)$$

According to our measurements for collagen solutions capable of undergoing MDT the difference $\sigma_{w2} - \sigma_{w1}$ was 3–4 dyn/cm,²⁵ whereas the velocity of translocation v was of the order of 10^{-3} cm/s.²⁰ The results on η , reported in this work, together with Eq. (8) then imply that MDT can plausibly be driven by interfacial forces as long as $\eta < 10^3$ Poise. The viscosity reaches this value in about 3 min after the lag phase ends.

In conclusion, our measurements on the viscous properties of collagen solutions used in MDT indicate that, as previously suggested, these matrices are capable of being rearranged by the available surface and interfacial forces during the first few minutes of their assembly. Our data, moreover, indicate the presence of organizational differences in particle-containing and -lacking collagen matrices from the earliest stages of the assembly process, which may bear on the apparent phase separation observed in the MDT experiment. More generally, the results presented here contribute to a further understanding of the nucleation and assembly events that take place during collagen fibrillogenesis.

Two of us acknowledge the support of the National Science Foundation under grants NSF IBN 93-17633 (GF) and NSF IBN 93-05628 (SAN).

REFERENCES

1. Hay, E. D., Ed. (1991) *Cell Biology of the Extracellular Matrix*, 2nd ed., Plenum Press, New York.
2. Birk, D. E., Zycband, E. I., Winkelmann, D. A. & Trelstad, R. L. (1988b) *Proc. Natl. Acad. Sci. USA* **86**, 4549–4553.
3. Veis, A. & George, A. (1994) in *Extracellular Matrix-Assembly and Structure*, Yurchenco, P. D., Birk, D. E. & Mecham, R. P., Eds., Academic Press, London, pp. 15–45.
4. Flory, P. J. (1973) *Principles of Polymer Chemistry*, Cornell University Press, Ithaca, NY.
5. Sahimi, M. (1994) *Applications of Percolation Theory*, Taylor and Francis, London.
6. Forgacs, G., Jaikaria, N. S., Frisch, H. L. & Newman, S. A. (1989) *J. Theor. Biol.* **140**, 417–430.

7. Forgacs, G., Newman, S. A., Obukhov, S. P. & Birk, D. E. (1991) *Phys. Rev. Lett.* **67**, 2399–2402.
8. Comper, W. D. & Veis, A. (1977) *Biopolymers* **18**, 2113–2131.
9. Comper, W. D. & Veis, A. (1977) *Biopolymers* **18**, 2133–2142.
10. Suarez, G., Veliz, M. & Nagel, R. L. (1980) *Arch. Biochem. Biophys.* **205**, 422–427.
11. Suarez, G., Oronsky, A. L., Bordas, J. & Koch, M. H. J. (1985) *Proc. Natl. Acad. Sci. USA* **82**, 4693–4696.
12. Brokaw, J. L., Doillon, C. J., Hahn, R. A., Birk, D. E., Berg, R. A. & Silver, F. H. (1985) *Int. J. Biol. Macromol.* **7**, 135–140.
13. Farber, S., Garg, A. K., Birk, D. E. & Silver, F. H. (1986) *Int. J. Biol. Macromol.* **8**, 37–42.
14. Steinberg, M. S. (1978) in *Specificity of Embryological Interactions*, Garrod, D., Ed., Chapman and Hall, London, pp. 97–130.
15. Steinberg, M. S. & Poole, T. J. (1982) in *Cell Behavior*, Bellairs, R., Curtis, A. S. G. & Dunn, G., Eds., Cambridge University Press, Cambridge, pp. 583–607.
16. Armstrong, P. B. (1989) *Crit. Rev. Biochem. Mol. Biol.* **24**, 119–149.
17. Steinberg, M. S. & Takeichi, M. (1994) *Proc. Natl. Acad. Sci. USA* **91**, 206–209.
18. Foty, R. A., Forgacs, G., Pflieger, C. M. & Steinberg, M. S. (1994) *Phys. Rev. Lett.* **72**, 2298–2301.
19. Foty, R. A., Pflieger, C. M., Forgacs, G. & Steinberg, M. S. (1996) *Development* **122**, 1611–1620.
20. Newman, S. A., Frenz, D. A., Tomasek, J. J. & Rabbuzzi, D. D. (1985) *Science* **228**, 885–889.
21. Newman, S. A., Frenz, D. A., Hasegawa, E. & Akiyama, S. K. (1987) *Proc. Natl. Acad. Sci. USA* **84**, 4791–4795.
22. De Gennes, P. G. (1985) *Rev. Mod. Phys.* **57**, 827–863.
23. De Gennes, P. G. (1979) *Scaling Concepts in Polymer Physics*, Cornell University Press, Ithaca, NY.
24. Li, D. & Neumann, A. W. (1993) *Langmuir* **9**, 50–54.
25. Forgacs, G., Newman, S. A., Polikova, Z. & Neumann, W. (1994) *Coll. Surf. B: Biointerf.* **3**, 139–146.
26. De Gennes, P. G. (1976) *J. Phys.* **37**, L1–L2.
27. Gauthier-Manuel, B., Meyer, R. & Pieranski, P. (1984) *J. Phys. E: Sci. Instrum.* **17**, 1177–1186.
28. Adam, M., Delsanti, M., Pieranski, P. & Meyer, R. (1984) *Rev. Phys. Appl.* **19**, 253–264.
29. Adam, M., Delsanti, M. & Durand, D. (1985) *Macromolecules* **18**, 2285–2290.
30. Allain, C. & Salomé, L. (1990) *Macromolecules* **23**, 981–987.
31. Wood, G. C. & Keech, M. K. (1960) *Biochem. J.* **75**, 588–698.
32. Djabourov, M. & Papon, P. (1983) *Polymers* **24**, 537–542.
33. Campbell, G. A. & Forgacs, G. (1990) *Phys. Rev.* **A41**, 4570–4573.
34. Fougnot, C., Jozefowicz, M. & Rosenberg, R. D. (1984) *Biomaterials* **5**, 94–99.
35. McPherson, J. M., Sawamura, S. J., Condell, R. A., Rhee, W. & Wallace, D. G. (1988) *Collagen Rel. Res.* **1**, 65–82.
36. Jeffrey, D. J. & Acrivos, A. (1976) *AIChE J.* **22**, 417–432.
37. Thomas, D. G. (1965) *J. Colloid Sci.* **20**, 267–277.
38. Perrot, F., Guenoun, P., Baumberger, T., Beysens, D., Garrabos, Y. & Le Neindre, B. (1994) *Phys. Rev. Lett.* **73**, 688–691.
39. Piez, K. A. (1975) in *Extracellular Matrix Influences on Gene Expression*, Slavkin, H. C. & Gruelich, R. C., Eds., Academic Press, New York, pp. 231–236.